RSC Advances

PAPER

View Article Online
View Journal | View Issue

Cite this: *RSC Adv.*, 2025, **15**, 12785

In-source photocatalytic fragmentations of oligosaccharides in surface-assisted laser desorption/ionization mass spectrometry over titania nanoparticles

Takashi Fujita [a] and Kohei Shibamoto *[b]

Received 7th February 2025
Accepted 8th April 2025

DOI: 10.1039/d5ra00898k

rsc.li/rsc-advances

In this study, we investigated the fragmentation behavior of oligosaccharides, specifically α-cyclodextrin (α-CD) and maltohexaose, using TiO_2 nanoparticles as ionizing substrates in SALDI-MS. Both compounds exhibited selective fragmentation at glycosidic bonds, with characteristic fragment ions for α-CD observed at m/z = 835, 673, 511, and 349. Similar fragmentation patterns were obtained with other metal oxide semiconductors (ZnO, Fe_2O_3, WO_3), while non-oxide semiconductors (CdS, CdSe) showed no fragmentation or molecular ion signals. The suppression of fragmentation upon glucose addition suggests the involvement of photoinduced holes, indicating that charge separation and oxide properties of the substrate contribute to the reaction. These findings demonstrate that SALDI-MS using oxide semiconductors enables controlled fragmentation of oligosaccharides and offers potential for structural analysis of glycans and photocatalytic surface reaction studies.

Introduction

Photocatalytic reactions mediated by semiconductor surfaces are highly beneficial for various applications, including organic degradation and organic synthesis.[1–3] These reactions occur when electron–hole pairs are generated through interband transitions in the semiconductor, facilitating redox reactions with chemical species adsorbed on its surface. The chemical reactions involving adsorbed organic materials are particularly diverse and complex. For example, even in the case of methylene blue, which is often studied in photocatalytic degradation, the intermediates are complex, and the degradation mechanism is difficult to elucidate at the molecular level.[4,5] Elucidating the reaction mechanism of photocatalysis will contribute to the design and improvement of efficient catalytic materials, optimization of reaction conditions, and development of new reactions. Therefore, developing analytical methods that can easily track intermediate products of photocatalytic reactions is crucial.

In situ infrared (IR) spectroscopy has been employed to analyze intermediates in photocatalytic reactions.[5,6] However, while IR spectroscopy can provide signals offering partial insights into molecular structures, interpretation of these signals can be complex. Thus, a complementary approach that allows direct detection of molecular fragments formed during photoinduced processes is highly desirable.

Surface-assisted laser desorption/ionization mass spectrometry (SALDI-MS) uses a pulsed laser to photoexcite a surface of an inorganic nanostructure, which serves as an ionizing substrate, to desorb and ionize molecules adsorbed on its surface for mass spectrometric analysis.[7–9] A commonly proposed mechanism for SALDI-MS involves rapid heating of the ionization substrate *via* laser irradiation, thus transferring internal energy to sample molecules for desorption and ionization. Therefore, it is important to control their optical, structural, and thermal properties to develop high-performance SALDI substrates. Various materials have been proposed as substrates for SALDI-MS, including metals, metal oxides, and carbon.[10–12] Among the metal oxides, nanostructured TiO_2 is frequently used as a substrate for SALDI-MS owing to its excellent UV absorbance, high chemical stability, and high specific surface area.[13,14]

In 2008, Qiao *et al.* demonstrated that the incorporation of TiO_2 into a MALDI matrix could induce peptide photooxidation through laser-activated photocatalytic reactions, thereby enabling sequence-specific fragmentation during MS analysis.[15] These results suggested that photocatalytic processes can occur within a single laser pulse and be captured in the mass spectrum. More recently, an on-plate reaction strategy has been developed, wherein drug molecules are photooxidized on a TiO_2 surface under UV irradiation and subsequently react with glutathione.[16] This approach illustrates the potential of TiO_2 to

[a]*Department of Applied Chemistry, School of Engineering, Tokyo University of Technology, 1401-1 Katakura, Hachioji, Tokyo 192-0982, Japan*

[b]*Department of Chemistry, Graduate School of Science, Tokyo Metropolitan University, 1-1 Minami-Osawa, Hachioji, Tokyo 192-0397, Japan. E-mail: shiba@tmu.ac.jp; Tel: +81-42-677-2531*

function as a photochemical microreactor for analytical applications.

In our previous studies on the development of ionization substrates for SALDI-MS, we focused on the role of charge transfer between sample molecules and photoexcited substrates.[17–20] We demonstrated that when gold nanoparticles (NPs) are used as ionization substrates, energy transfer from the substrate to the analyte *via* localized surface plasmon resonance enhances the efficiency of desorption and ionization.[17–19] These results indicate that charge interactions between photoexcited substrates and analyte molecules can significantly affect the resulting mass spectra.

Building on this concept, we analyzed α-cyclodextrin (α-CD) using a pulsed ultraviolet laser with TiO_2 nanoparticle substrates and observed a series of regular fragment ions corresponding to the cleavage of individual glucose units.[20] These fragments differed from those generated using non-photocatalytic substrates such as surface-roughened silicon, or under high-power laser conditions in MALDI-MS. While these findings implied a possible involvement of photocatalytic activity in the fragmentation process, the underlying mechanism remains unclear.

In this study, we aim to elucidate the factors governing selective fragmentation of oligosaccharides in SALDI-MS using TiO_2 NPs. We focus on the influence of semiconductor type—comparing oxide (TiO_2, ZnO, Fe_2O_3, WO_3) and non-oxide (CdS, CdSe) materials—on the fragmentation behavior of α-CD and maltohexaose. Additionally, we examine the effect of hole scavengers such as glucose to assess the role of photogenerated charge carriers in the fragmentation process. By systematically investigating the relationship between material properties and fragmentation behavior, this study provides insights into the interplay between photocatalytic surface processes and mass spectrometric fragmentation, expanding the potential of SALDI-MS as a tool for surface photochemistry analysis.

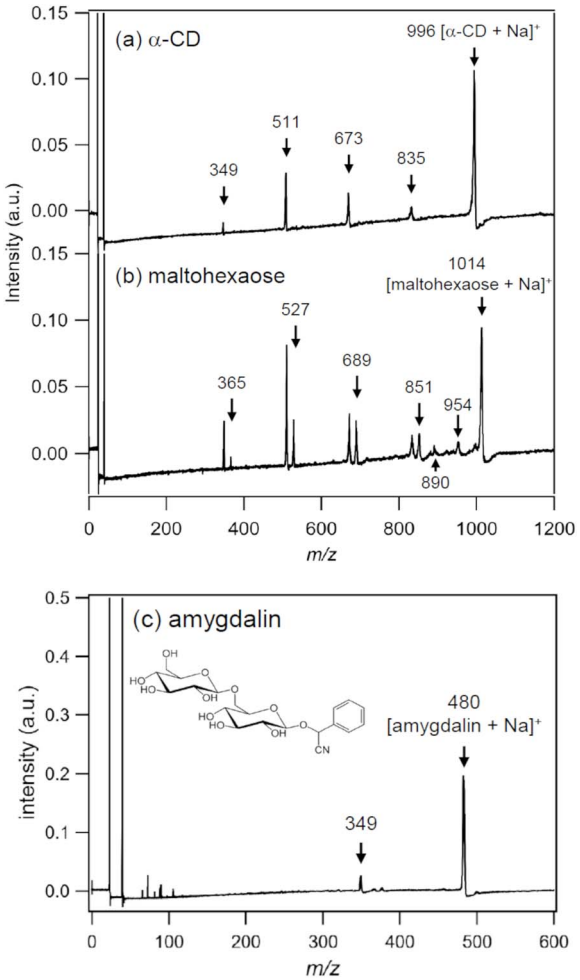

Fig. 1 Mass spectra obtained using TiO_2 NPs as the ionizing substrate for (a) α-CD, (b) maltohexaose, and (c) amygdalin in the positive ion mode. Each compound was applied at a concentration of 1 nmol onto the ionizing substrate. Excitation was performed with a pulsed laser at a wavelength of 266 nm.

Results and discussion

Fig. 1 shows the mass spectra obtained using TiO_2 NPs as a ionizing substrate for (a) α-CD, (b) maltohexaose, and (c) amygdalin in a positive ion mode with an excitation wavelength of 266 nm. Strong signals detected at $m/z = 23$ and 39 in all spectra were attributed to Na^+ and K^+, respectively. In the spectrum of α-CD, a peak corresponding to the $[\alpha\text{-CD} + Na]^+$ ion was detected at $m/z = 996$. Additional peaks were observed at $m/z = 835$, 673, 511, and 349. The m/z difference between these peaks is 162, which corresponds to glycosyl group. These peaks therefore correspond to the fragment ions of α-CD, specifically $[\text{pentasaccharide} + Na - 16]^+$, $[\text{tetrasaccharide} + Na - 16]^+$, $[\text{trisaccharide} + Na - 16]^+$, and $[\text{disaccharide} + Na - 16]^+$, respectively. The regular fragmentation pattern of this mass spectrum follows our previously reported findings.[20] In the spectrum of maltohexaose, a peak was observed at $m/z = 1014$, attributed to $[\text{maltohexaose} + Na]^+$. Furthermore, fragment ions of maltohexaose were observed at $m/z = 851$, 835, 689, 673, 527, 511, 365, and 349, which were attributed to $[\text{pentasaccharide} + Na - 16]^+$, $[\text{tetrasaccharide} + Na]^+$, $[\text{tetraose} + Na - 16]^+$, $[\text{trisaccharide} + Na]^+$, $[\text{trisaccharide} + Na - 16]^+$, $[\text{disaccharide} + Na]^+$, and $[\text{disaccharide} + Na - 16]^+$, respectively, based on the m/z values. Even though the Na^+ adduct of the monosaccharide was expected at $m/z = 203$, it was not observed. Peaks observed at $m/z = 954$ and 890 were presumed to be ion species resulting from fragmentation of carbon chains in maltohexaose consisting of four and two carbon atoms, respectively.

Single fragment ions were observed in α-CD at 16 m/z units lower compared to the sodium adducts of each oligosaccharide unit. Conversely, the oligosaccharide unit of maltohexaose and fragment ions similar to those of α-CD exhibited fragment ions with m/z values of 16 units higher. Molecular structure of maltohexaose is linear, whereas that of α-CD is cyclic; the 16 m/z difference is attributed to the oxygen atoms in the glycosidic bonds. Based on this mass spectral data, the fragmentation process was deduced: in α-CD, initial fragmentation leads to ring opening, followed by a second fragmentation producing the fragments observed in Fig. 1(a). These fragments contain a glycosidic bond with an oxygen atom on one side and are

observed as ions upon Na^+ addition. In maltohexaose, cleavage results in two types of fragments, one with oxygen atoms on one side and the other on both sides, leading to two distinct fragment ions for each saccharide unit. This result indicates that the characteristic fragmentation pattern of oligosaccharides in SALDI-MS with TiO_2 happens selectively at the glycosidic bond connecting the saccharide units. Moreover, if this fragmentation is due to hydrolysis, at least two ion peaks should be observed because of H or OH addition to the α-CD cleavage site. However, only one α-CD fragment was observed in this experiment. Therefore, this selective fragmentation is thought to occur *via* a different process than hydrolysis.

To confirm this fragmentation, amygdalin molecules were analyzed under similar conditions, as presented in Fig. 1(c). At $m/z = 480$, an ion peak corresponding to Na^+ adduct of amygdalin molecule was observed. Additionally, a fragment ion was noted at $m/z = 349$. The molecular structure of amygdalin includes two sugar molecules and mandelonitrile. The ion at $m/z = 349$ corresponds to the $[\text{disaccharide} + Na]^+$ ion, resulting from the fragmentation of amygdalin into two sugar molecules and mandelonitrile. This suggests that fragmentation occurs at the oxygen atom bridging mandelonitrile and disaccharide moiety.

These results indicate that SALDI-MS using TiO_2 NPs induces specific fragmentation at the glycosidic bonds, specifically at the C–O–C linkages within the sugar molecules. However, as observed in the measurements of α-CD and maltohexaose, no fragment ions derived from monosaccharides were detected.

Fig. 2 shows the positive ion mode mass spectra of α-CD using (a) ZnO, (b) Fe_2O_3, (c) WO_3, (d) CdS, and (e) CdSe as ionized substrates in the positive ion mode with an excitation wavelength of 266 nm. Band gaps of these semiconductor materials were 3.43 eV for ZnO, 2.3 eV for Fe_2O_3, 2.6 eV for WO_3, 2.42 eV for CdS, and 1.7 eV for CdSe.[21–23] Given that the photon energy of 266 nm light corresponds to approximately 4.66 eV, interband excitation is energetically feasible for all these semiconductors, including ZnO, which possesses the widest bandgap among them. When ZnO, Fe_2O_3, and WO_3 were used, the $[\alpha\text{-CD} + Na]^+$ ion and fragment ion peaks at $m/z = 835$, 673, 511, and 349 were similar to those observed with TiO_2. In addition, Fe_2O_3 exhibited peaks at $m/z = 89$ and 105, which were difficult to attribute. Similarly, WO_3 exhibited multiple peaks in the range of approximately 280–400, which were also difficult to attribute. These are thought to be either ions derived from the substrate material used or fragment ions of α-CD. When using CdS or CdSe as ionization substrates, the ions of $[\alpha\text{-CD} + Na]^+$ and the cleavage ions detected with TiO_2 were not observed at any laser fluence. Instead, Cd^+ ions at $m/z = 112$ and Cd_2^+ ions at $m/z = 224$ were observed. Additionally, with CdSe, five unidentified ion peaks appeared at $m/z = 392$, 472, 551, 629, and 708. The m/z values of these peaks differ from both the molecular weight of $[\alpha\text{-CD} + Na]^+$ and the fragment ions detected in TiO_2. The 79-unit difference in m/z among the peaks at $m/z = 472$, 551, 629, and 708 suggests that they may be attributed to clusters containing multiple Se atoms, each with an atomic weight of 79.

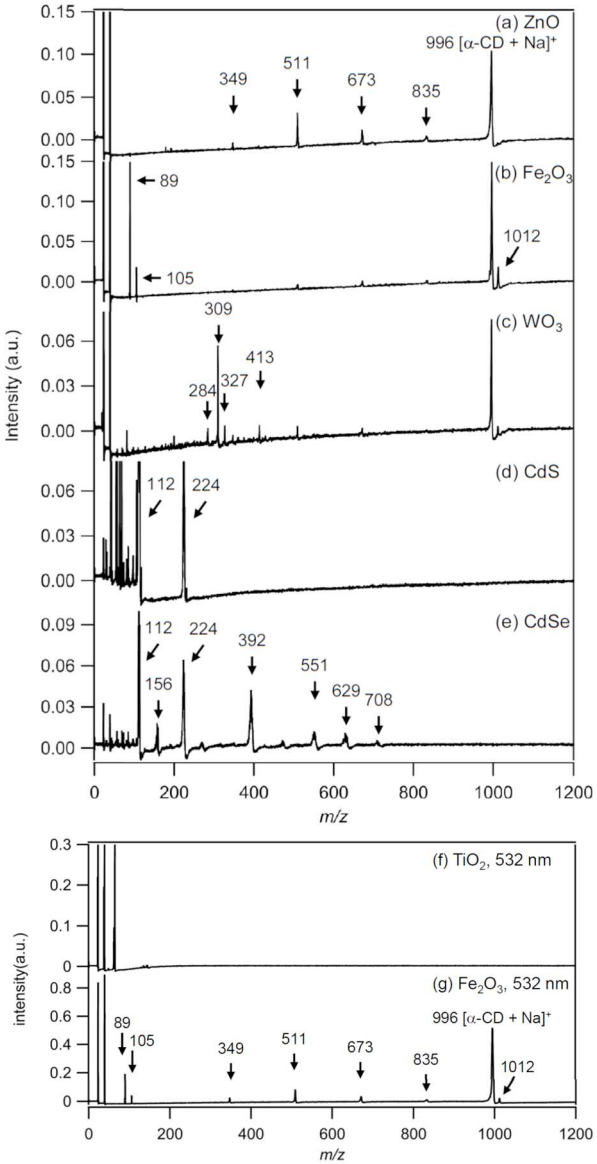

Fig. 2 Mass spectra of α-cyclodextrin (α-CD) obtained using different ionization substrates: (a) ZnO, (b) Fe_2O_3, (c) WO_3, (d) CdS, and (e) CdSe in the positive ion mode, recorded at an excitation wavelength of 266 nm. Mass spectrum of α-CD using (f) TiO_2, and (g) Fe_2O_3 recorded at an excitation wavelength of 532 nm.

These results demonstrate that selective fragmentation of α-CD occurs on oxide semiconductor substrates such as ZnO, Fe_2O_3, WO_3, and TiO_2, whereas neither fragmentation nor intact α-CD ion signals were observed with non-oxide semiconductors such as CdS and CdSe. Although the detailed mechanism remains unclear, the findings suggest that lattice oxygen and photoinduced charge separation in oxide semiconductors are critical factors promoting fragmentation.

Fe_2O_3, with a band gap of 2.5 eV, can be excited using the second harmonic of a Nd:YAG laser with a wavelength of 532 nm. Fig. 2(g) presents a mass spectrum of α-CD obtained *via* pulsed laser excitation at 532 nm using Fe_2O_3 as the ionization substrate. The observed ions include $[\alpha\text{-CD} + Na]^+$ and fragment

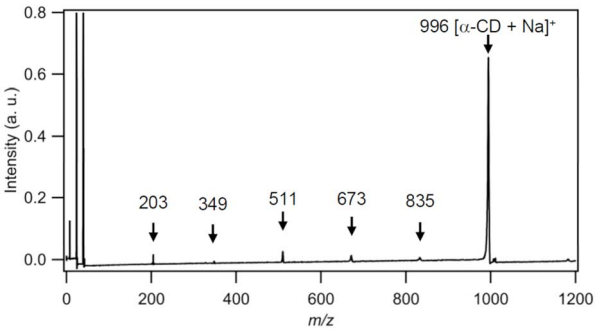

Fig. 3 Mass spectra of α-CD + glucose obtained using TiO_2 NPs as the ionizing substrate. Each compound was applied at a concentration of 1 nmol onto the ionizing substrate. Excitation was performed with a pulsed laser at a wavelength of 266 nm.

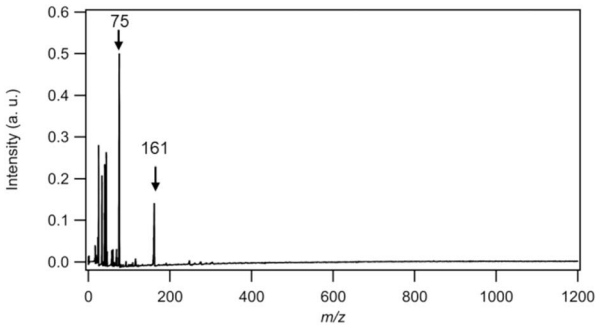

Fig. 4 Negative ion mode mass spectra of α-CD obtained using TiO_2 NPs as the ionizing substrate. α-CD was applied at a concentration of 1 nmol onto the ionizing substrate. Excitation was performed with a pulsed laser at a wavelength of 266 nm.

ions from sugar units, which is consistent with the results obtained at a wavelength of 266 nm. However, when TiO_2, which has a wider band gap than 532 nm, was used with the 532 nm pulsed laser, no α-CD-related peaks were detected at any laser intensity, as shown in Fig. 2(f). These results suggest that charge separation in oxide semiconductors based on interband transitions play a significant role in the fragmentation of oligosaccharides in SALDI-MS. When Fe_2O_3 was employed as the ionization substrate, a higher number of ions were observed under excitation at 532 nm compared to 266 nm, despite using the same laser fluence. Although the exact cause of this difference remains unclear, it is hypothesized that the absorbance of Fe_2O_3 at 266 nm might be lower than at 532 nm.[24]

The absence of the $[\text{monosaccharide} + \text{Na}]^+$ ion at $m/z = 203$ during the analysis of α-CD remains unexplained. To further investigate this, an equimolar mixture of glucose and α-CD was prepared and analyzed using SALDI-MS. Fig. 3 presents the mass spectrum of a mixed sample containing 1 nM α-CD and 1 nM D-glucose, measured at an excitation wavelength of 266 nm using a TiO_2 NPs. Upon glucose addition, the undissociated $[\alpha\text{-CD} + \text{Na}]^+$ ion exhibited a strong signal intensity of 0.65 at $m/z = 996$, compared to 0.10 observed for the $[\alpha\text{-CD} + \text{Na}]^+$ ion in the absence of glucose (Fig. 1(a)).

Compared to the α-CD spectrum in Fig. 1(a), only a minimal amount of fragment ions deriving from the undissociated ion was observed, despite the same irradiation laser fluence. This finding suggests that glucose suppresses the characteristic fragmentation of α-CD. Moreover, despite the equimolar addition of glucose, the ion peak for $[\text{glucose} + \text{Na}]^+$ at $m/z = 203$ was scarcely detected. In photocatalysis, glucose is known to act as a hole-scavenging molecule.[25] Given the charge separation properties of TiO_2, it is plausible that the added glucose, or monosaccharides produced *via* cleavage by TiO_2, preferentially consumed holes, resulting in the reduced formation of $[\text{monosaccharide} + \text{Na}]^+$ ions at $m/z = 203$. Previous studies on SALDI-MS using TiO_2 NPs surface have not reported the characteristic fragments observed in this study. A possible explanation is that many SALDI-MS experiments incorporate additives, such as cationizing agents, which may function as hole scavengers, thereby suppressing fragment formation. Indeed, our previous study indicated that citric acid, a commonly used cationizing agent, exhibits a fragment-suppressing effect.[20]

To explore the possibility that monosaccharide ions generated by hole-induced reactions may form negative ions, α-CD was measured in negative ion mode using TiO_2 NPs as the ionization substrate under 266 nm excitation, as shown in Fig. 4.

Ion peaks were observed at $m/z = 75$ and 161, with additional peaks in the m/z range of 16–70. The peak at $m/z = 161$ was assigned to $[C_6H_{10}O_5]^-$, likely formed by the loss of H_2O and H^+ from glucose. The peak at $m/z = 75$ was attributed to $[C_3H_7O_2]^-$. These anions approximately match the fragmentation patterns of sugars obtained using inductively coupled plasma and electrospray ionization.[26] The peaks in the m/z range of 16–70 were difficult to assign but were not detected without α-cyclodextrin (α-CD), suggesting they are fragments generated through the dehydrative decomposition or partial oxidation of saccharides. From this result, it is suggested that the absence of monosaccharide ions in the positive ion mode was due to their ionization in the negative ion mode.

The limitations of this study include its focus on material composition and α-CD fragmentation, without detailed consideration of particle size. Standardizing particle size is crucial for a more rigorous evaluation of desorption/ionization efficiency and surface reactivity. Although CdS and CdSe substrates did not yield α-CD ions or fragments, the influence of particle size cannot be excluded, as smaller particles generally enhance desorption and ionization efficiency in LDI-based techniques. In addition to particle size, the chemical activity of semiconductor substrates is influenced by multiple physicochemical properties, including surface area, crystal phase, exposed facets, and aggregation state. Therefore, achieving full standardization and direct comparison of different materials is inherently challenging. Another factor to consider is the sample concentration: the 1 nM condition likely resulted in multilayer molecular coverage, which may have enhanced signal intensity but reduced surface specificity. Performing measurements under monolayer conditions would provide more precise insight into surface–molecule interactions.

Experimental

TiO_2 NPs P25 were obtained from AEROSIL Japan. Ionized substrates with TiO_2 NPs were prepared using our previously reported method with some modifications.[19,20,27] The TiO_2 NPs were sonicated in ion-exchange water to create a suspension suitable for ionization. An equal volume of toluene was added to form a water/oil interface, followed by the vigorous injection of methanol, resulting in the formation of a TiO_2 NPs thin film at the interface. The film was carefully transferred to a silicon substrate provided by Niraco, rinsed with distilled water, air-dried at room temperature, and used for SALDI-MS analysis after applying the sample solution.

ZnO, Fe_2O_3, WO_3, CdS and CdSe were used as ionizing substrates for comparison with TiO_2. ZnO, Fe_2O_3, and WO_3, with primary particle sizes of 100 nm, 1 μm, and less than 50 nm, respectively, were purchased from Wako. CdS and CdSe, with primary particle sizes of 1 μm and less than 10 μm, respectively, were purchased from Sigma-Aldrich. For semiconductors other than TiO_2 NPs, a suspension was created *via* ultrasonicating in ion-exchanged water, followed by placement onto the silicon substrate. After drying, the substrate was subjected to LDI-MS analyses.

Regarding the sample molecules, α-CD and maltohexaose were dissolved in ion-exchanged water to yield a 1 mM solution. This sample solution (1 μL) was dropped onto an ionized substrate and dried for LDI-MS measurements.

The ionization substrates were introduced into a linear time-of-flight (TOF) mass spectrometer developed in our laboratory, equipped with a delayed extraction ion source. The acceleration voltage ranged from 4.0 to 3.0 kV, and the mass spectra were acquired in the positive ion mode. Nd: a YAG pulsed laser with fourth harmonic generation (FHG, $\lambda = 266$ nm, 8 ns pulse width, and 10 Hz frequency) was utilized as the excitation source. The laser beam was focused onto the target surface using an optical lens, resulting in a spot diameter of 0.17 mm. The laser fluence was adjusted to a marginally higher intensity than the threshold required for ionizing the sample molecules. The mass spectra were obtained *via* integration of 64 shots.

Conclusions

In this study, we investigated the fragmentation behavior of oligosaccharides, specifically α-cyclodextrin (α-CD) and maltohexaose, using TiO_2 nanoparticles as ionizing substrates in SALDI-MS. Both compounds exhibited selective fragmentation at glycosidic bonds, with characteristic fragment ions at m/z = 835, 673, 511, and 349 for α-CD. Similar fragmentation patterns were observed with other metal oxide semiconductors (ZnO, Fe_2O_3, WO_3), but not with non-oxide semiconductors (CdS, CdSe). The addition of equimolar glucose significantly suppressed fragmentation, indicating its role as a hole scavenger and underscoring the importance of photoinduced charge separation in the process. These results suggest that both the semiconductor being an oxide and its ability to undergo interband excitation may play important roles in promoting oligosaccharide fragmentation, potentially *via* photocatalytic surface reactions. Overall, the method shows promise for investigating photocatalytic surface reactions and enables structural analysis of glycan-type molecules with high molecular specificity, thereby broadening the applicability of SALDI-MS in surface chemistry and biomolecular research.

Data availability

All data supporting the findings of this study are included within the article.

Author contributions

The manuscript was written through contributions of all authors. All authors have given approval to the final version of the manuscript.

Conflicts of interest

There are no conflicts to declare.

Acknowledgements

This work was supported by JSPS KAKENHI Grant Numbers JP24K08058 and JP18K04730 (Kohei Shibamoto) and JP24K08186 (Takashi Fujita).

Notes and references

1 A. Fujishima, X. Zhang and D. A. Tryk, *Surf. Sci. Rep.*, 2008, **63**, 515–582.
2 A. Kubacka, M. Fernandez-García and G. Colón, *Chem. Rev.*, 2012, **112**, 1555–1614.
3 D. Friedmann, A. Hakki, H. Kim, W. Choi and D. Bahnemann, *Green Chem.*, 2016, **18**, 5391–5411.
4 A. Houas, H. Lachheb, M. Ksibi, E. Elaloui, C. Guillard and J. M. Herrmann, *Appl. Catal., B*, 2001, **31**, 145–157.
5 Z. Yu and S. S. C. Chuang, *Appl. Catal., B*, 2008, **83**, 277–285.
6 E. Moctezuma, E. Leyva, C. A. Aguilar, R. A. Luna and C. Montalvo, *J. Hazard. Mater.*, 2012, **243**, 130–138.
7 K. P. Law and J. R. Larkin, *Anal. Bioanal. Chem.*, 2011, **399**, 2597–2622.
8 Y. E. Silina and D. A. Volmer, *Analyst*, 2013, **138**, 7053–7065.
9 S. A. Iakab, P. Rafols, M. García-Altares, O. Yanes and X. Correig, *Adv. Funct. Mater.*, 2019, **29**, 1903609.
10 X. N. Wang and B. Li, *Anal. Chem.*, 2022, **94**, 952–959.
11 M. O. Amin, M. Madkour and E. Al-Hetlani, *Anal. Bioanal. Chem.*, 2018, **410**, 4815–4827.
12 X. Wang, S. Dou, Z. Wang, J. Du and N. Lu, *Microchim. Acta*, 2020, **187**, 161.
13 C. Gao, D. Zhen, N. He, Z. An, Q. Zhou, C. Li, C. A. Grimes and Q. Cai, *Talanta*, 2019, **196**, 1–8.
14 C. Gao, Y. Wang, H. Zhang and W. Hang, *Anal. Chem.*, 2023, **95**, 650–658.
15 L. Qiao, J. Wan, J. Kong, P. Yang and B. H. Liu, *Angew. Chem., Int. Ed.*, 2008, **47**, 2646–2648.

16 O. A. Keltsieva, A. A. Afanasyeva, M. A. Slyusarenko, S. K. Ilyushonok, A. S. Gladchuk, Y. S. Nitsulenko, Y. K. Kalninia, I. E. Perevoznikov, N. Y. Rogovskaya, A. A. Selyutin, A. S. Frolov, A. N. Arseniev, A. Y. Gorbunov, A. S. Kovalenko, A. M. Nikolaev, V. N. Babakov, K. A. Krasnov and E. P. Podolskaya, *Microchem. J.*, 2025, **208**, 112377.
17 K. Shibamoto, K. Sakata, K. Nagoshi and T. Korenaga, *J. Phys. Chem. C*, 2009, **113**, 17774–17779.
18 K. Shibamoto, Y. Nishimura and T. Fujita, *Chem. Lett.*, 2016, **45**, 262–264.
19 K. Shibamoto and T. Fujita, *ACS Omega*, 2024, **9**, 21822–21828.
20 T. Fujita and K. Shibamoto, *Chem. Lett.*, 2013, **42**, 852–853.
21 M. Mishra and D. M. Chun, *Appl. Catal., A*, 2015, **498**, 126–141.
22 P. P. González-Borrero, F. Sato, A. N. Medina, M. L. Baesso, A. C. Bento, G. Baldissera, C. Persson, G. A. Niklasson, C. G. Granqvist and A. Ferreira da Silva, *Appl. Phys. Lett.*, 2010, **96**, 061909.
23 A. S. Khomane, *J. Alloys Compd.*, 2010, **506**, 849–852.
24 S. Mitra, S. Das, K. Mandal and S. Chaudhuri, *Nanotech*, 2007, **18**, 27.
25 I. A. Shkrob, M. C. Sauer and D. Gosztola, *J. Phys. Chem. B*, 2004, **108**, 12512–12517.
26 V. F. Taylor, R. E. March, H. P. Longerich and C. J. Stadey, *Int. J. Mass Spectrom.*, 2007, **21**, 1165–1175.
27 T. Fujita and K. Shibamoto, *ACS Omega*, 2022, **7**, 44711–44719.